Proteomic Analysis of Embryonic and Young Human Vitreous

Kenneth M. P. Yee,[1,2] Edward P. Feener,[3] Michele Madigan,[4,5] Nicholas J. Jackson,[6] Ben-Bo Gao,[3] Fred N. Ross-Cisneros,[2] Jan Provis,[7,8] Lloyd Paul Aiello,[3,9] Alfredo A. Sadun,[2,10] and J. Sebag[1,2]

[1]VMR Institute for Vitreous Macula Retina, Huntington Beach, California, United States
[2]Doheny Eye Institute, Los Angeles, California, United States
[3]Beetham Eye Institute, Joslin Diabetes Center, Boston, Massachusetts, United States
[4]School of Optometry and Vision Science, University of New South Wales, Sydney, Australia
[5]Save Sight Institute, University of Sydney, Sydney, Australia
[6]Department of Medicine Statistics Core, David Geffen School of Medicine at UCLA, Los Angeles, California, United States
[7]John Curtin School of Medical Research, Canberra, Australia
[8]Australian National University, Canberra, Australia
[9]Department of Ophthalmology, Harvard Medical School, Boston, Massachusetts, United States
[10]Department of Ophthalmology, David Geffen School of Medicine at UCLA, Los Angeles, California, United States

PURPOSE. The proteomic profile of vitreous from second-trimester human embryos and young adults was characterized using mass spectrometry and analyzed for changes in protein levels that may relate to structural changes occurring during this time. This vitreous proteome was compared to previous reports to confirm proteins already identified and reveal novel ones.

METHODS. Vitreous from 17 human embryos aged 14 to 20 weeks gestation (WG) and from a 12-, a 14-, a 15-, and a 28-year-old was individually analyzed using tandem mass spectrometry–based proteomics. Peptide spectral count associations with embryonic age were assessed using a general linear model of fold changes and Spearman's rank correlation. Differences between embryonic and young adult vitreous proteomes were also compared. Immunohistochemistry was used to evaluate three proteins in five additional fetal (10–18 WG) human eyes.

RESULTS. There were 1217 proteins identified in fetal and young adult human vitreous, 206 after quantile normalization and variance filtering. In embryos, the peptide counts of 37 proteins changed significantly from 14 to 20 WG: 75.7% increased, 24.3% decreased. Immunohistochemistry confirmed the absence of clusterin and cadherin in 10 and 14 WG eyes and their presence at 18 WG. Comparing embryonic to young adult vitreous, 47 proteins were significantly higher or lower. A total of 768 proteins not previously identified in the literature are presented.

CONCLUSIONS. Proteins previously unreported in the human vitreous were identified. The human vitreous proteome undergoes significant changes during embryogenesis and young adulthood. A number of protein levels change considerably during the second trimester, with the majority decreasing.

Keywords: vitreous, proteomics, embryology, vascular development

Vitreous is an important ocular tissue that undergoes extensive developmental change ultimately resulting in an optically clear tissue.[1,2] During the first trimester (1–12 weeks gestation [WG]) of ocular development, a complex vascular network composed of the hyaloid artery, the vasa hyaloidia propria, and the tunica vasculosa lentis develops within the vitreous body to nourish the developing eye, particularly the anterior segment and lens.[1,3] During the second trimester (approximately 13–26 WG) this hyaloid vasculature regresses, and by birth the vitreous body is a mostly acellular, optically clear gel.[4–7]

Proteomic analysis of vitreous has been previously used to investigate hyaloid regression in postnatal mice.[8,9] Proteomics have also been used to characterize vitreous in a variety of human diseases.[10–24] The Human Eye Proteome Project is a recent (2012) review and summary of the current status in proteomic studies of the eye.[25] This review identified 460 nonredundant human vitreous proteins in published literature. A more recent study identified 1205 proteins in normal human vitreous, 682 of which were previously unreported.[26] To date, proteomic studies of human embryonic vitreous have not been undertaken. The rationale to do so is that protein expression during this period of embryogenesis may be related to the significant structural changes occurring during this stage of vitreous development. The underlying hypothesis is that vitreous protein composition changes from 14 to 20 WG and differs at different fetal stages and in comparison to young adulthood.

METHODS

Study Design

This cross-sectional study analyzed the protein profiles of a series of postmortem human embryonic vitreous samples aged 14 to 20 WG ($N = 17$) and a 12-, a 14-, a 15-, and a 28-year-old. Five additional fetal eyes (10, 14, and 18 WG) were studied by immunohistochemistry.

Vitreous Origin and Storage

Vitreous was obtained from 26 eyes [ages: 10 ($n = 2$), 14 ($n = 3$), 15, 16, 17, 18, 18.5 ($n = 3$), 19 ($n = 3$), and 20 ($n = 4$) WG; and 12, 14, 15, and 28 years old]. Human fetal eyes were obtained at surgery to terminate pregnancy with maternal consent and ethical approval from the Human Ethics Committees of the University of Sydney and the University of New South Wales, in accordance with the tenets of the Declaration of Helsinki. Ultrasound and postmortem measurements of foot length were used to determine the gestational age. In all subjects, the vitreous was obtained within 2 to 4 hours post mortem. Only one vitreous body of each subject was employed in this study. The fellow eye was employed for unrelated studies of retinal embryology.

Eyes were examined at the time of dissection to confirm that there was no gross pathology in the anterior and posterior segments. Unfixed eyes were dissected with an initial incision made approximately 1 to 2 mm posterior to the limbus (depending on eye size), and then carefully extended around the limbus using microscissors, so as to remove the anterior eye structures (cornea, iris, and lens). The vitreous including hyaloid vessels was removed with the lens, which was subsequently removed during viewing with a dissecting microscope. For human fetal eyes, the vitreous can be readily removed from the eye cup as a "globule" or gel body. The entire vitreous was immediately placed in sterile Eppendorf tubes, snap-frozen, and stored at −80°C. No maternal or family history was available for those subjects other than the age in WG. The young adult eyes were obtained from the New England Eye Bank.

Vitreous Prefractionation and Proteomics

Fifty microliters of undiluted vitreous was separated by one-dimensional SDS-PAGE, and proteins were visualized using Coomassie Brilliant Blue G-250 stain (Bio-Rad, Hercules, CA, USA). Each sample/gel lane was cut into 40 slices, and proteins were subjected to in-gel digestion using trypsin (Promega, Madison, WI, USA). Tryptic peptides were analyzed by nanospray liquid chromatography-tandem mass spectrometry (LC-MS/MS) using a LTQ linear ion trap mass spectrometer (Thermo Scientific, San Jose, CA, USA) as described previously.[16,27] Proteins that were identified in at least two independent vitreous samples by a minimum of two peptides matched in the same or adjacent gel slices were reported. The total peptide-spectral matches for each of these reported proteins were compiled as a semiquantitative measure of protein abundance. Proteins with peptide counts below this detection threshold were considered zero concentrations.

Database Searching

All MS/MS samples were analyzed using X! Tandem (version X! Tandem Piledriver [2015.04.01.1]; The GPM, thegpm.org, in the public domain). X! Tandem was set up to search the uni.HUMANRevConcat.2015_03.fasta.pro database (March 2015; 179,818 entries) assuming the digestion enzyme trypsin. X! Tandem was searched with a fragment ion mass tolerance of 0.50 Da and a parent ion tolerance of 1.00 Da. Glu->pyro-Glu of the n-terminus, ammonia loss of the n-terminus, gln->pyro-Glu of the n-terminus, oxidation of methionine, and propionamide of cysteine were specified in X! Tandem as variable modifications.

Criteria for Protein Identification

Scaffold (version Scaffold_4.4.1.1; Proteome Software, Inc., Portland, OR, USA) was used to validate MS/MS-based peptide and protein identifications. Peptide identifications were accepted if they could be established at greater than 89.0% probability to achieve a false discovery rate (FDR) less than 0.5% by the Scaffold Local FDR algorithm. Protein identifications were accepted if they could be established at greater than 99.0% probability to achieve an FDR less than 1.0% and contained at least two identified peptides. Protein probabilities were assigned by the Protein Prophet algorithm.[28] Proteins that contained similar peptides and could not be differentiated based on MS/MS analysis alone were grouped to satisfy the principles of parsimony. Proteins were annotated with GO terms from the National Center for Biotechnology Information (downloaded April 24, 2015).[29]

Statistical Analyses

Spectral peptide counts were normalized using quantile normalization. A variance filtering procedure was applied such that proteins with zero values for >50% of their data within an age group were excluded from analysis. Age groups [early embryonic (14–18 WG, $N = 7$), late embryonic (19–20 WG, $N = 7$), and young adult (12, 14, 15 and 28 years old, $N = 4$)] were compared using a general linear model of the log values from the normalized data. Fold changes are presented. P values were adjusted for FDR using the Benjamini-Hochberg (BH) correction.[30] Spearman rank-order correlations were additionally conducted between the embryonic age and proteins. Analyses were conducted in Stata Version 13.1 (StataCorp LP; College Station, TX, USA).

Immunohistochemistry (IHC)

Dystroglycan and cadherin were found to undergo statistically significant change in peptide numbers from 14 to 20 WG, and clusterin similarly changed from the embryo to young adulthood. The commercial availability of human antibodies to these proteins enabled IHC evaluation in embryonic human eyes as previously described by our group.[31–33]

Five formalin-fixed, paraffin-embedded whole human eyes from embryos aged 10 ($n = 2$), 14 ($n = 2$), and 18 WG were used for histologic examination of the hyaloid vasculature. Immunohistochemistry experiments were performed in duplicate in the same eye and, when tissue was available, in multiple eyes of the same gestational age. Whole eye cups were processed and embedded in paraffin and serially sectioned at the horizontal meridian from cornea to optic nerve at 5 μm. Commercially available primary antibodies (Novus Biologicals, LLC, Littleton, CO, USA) directed against dystroglycan, cadherin, and clusterin were employed. Deparaffinization and rehydration were performed using a series of baths beginning with xylene, 100%, 95%, and 70% ethanol, with a final wash in distilled water. Antigen retrieval was performed using a sodium citrate buffer solution at pH 6.0 (Dako, Carpinteria, CA, USA) and heating under pressure in a microwave oven. The slides were rinsed and washed in a buffer (0.05 M Tris/HCl, 0.15 M NaCl, 0.05% Tween 20, pH 7.6) between each step of the IHC protocol. Three percent hydrogen peroxide was used for 10 minutes to block endogenous peroxidase. Rabbit anti-human primary polyclonal antibody for each protein was diluted to the

TABLE 1. Comparison of Embryonic Versus Young Adult Vitreous Proteins With FDR Adjusted *P* Values < 0.05

UniProtKB ID	%Δ	*P* FDR
ALDOA_HUMAN	−72	<0.001
H3BR04_HUMAN	−64	<0.001
PTGDS_HUMAN	−82	<0.001
A1AG1_HUMAN	−76	<0.001
K7EKH5_HUMAN	−83	<0.001
KAD1_HUMAN	−72	<0.001
PARK7_HUMAN	−59	<0.001
MDHC_HUMAN	−67	<0.001
PRDX6_HUMAN	−67	<0.001
TBAL3_HUMAN	−71	<0.001
H0Y7L5_HUMAN	−86	<0.001
APOE_HUMAN	−84	<0.001
A0A075B6N8_HUMAN	−82	<0.001
A0A0A0MS08_HUMAN	−72	<0.001
A0A0A0MSI0_HUMAN	−50	<0.001
A0A087WYC5_HUMAN	−73	<0.001
PGK1_HUMAN	−75	<0.001
DDAH1_HUMAN	−79	<0.001
UCHL1_HUMAN	−55	0.001
GPX3_HUMAN	−90	0.001
KPYM_HUMAN	−91	0.001
A1AG2_HUMAN	−68	0.001
CLUS_HUMAN	−80	0.001
PEDF_HUMAN	−87	0.001
IPYR_HUMAN	−62	0.001
A0A087WV47_HUMAN	−72	0.001
CBR1_HUMAN	−85	0.002
IGHG2_HUMAN	−84	0.002
OSTP_HUMAN	−64	0.002
DKK3_HUMAN	−70	0.002
TALDO_HUMAN	−54	0.002
A0A087X010_HUMAN	−65	0.003
A0A087X1C7_HUMAN	−66	0.003
LDHB_HUMAN	−39	0.005
CO4A_HUMAN	−67	0.007
J3QQX2_HUMAN	−54	0.008
X6RA14_HUMAN	−68	0.009
PGAM1_HUMAN	−57	0.010
PEA15_HUMAN	−57	0.016
OPT_HUMAN	−84	0.017
B4GA1_HUMAN	−78	0.019
G3V461_HUMAN	−77	0.022
H7BYH4_HUMAN	−56	0.029
TRFE_HUMAN	−49	0.031
TBA1B_HUMAN	−43	0.043
TBA1A_HUMAN	−43	0.043
F8VZY9_HUMAN	−81	0.045

Proteins are listed using Universal Protein Resource ID. The UniProt Knowledgebase (UniProtKB) is the central hub for the collection of functional information on proteins, with accurate, consistent, and rich annotation (http://www.uniprot.org/help/uniprotkb, in the public domain).

TABLE 2. Vitreous Proteins That Increased When Comparing Early (14–18 WG) Versus Late (19–20 WG) Second-Trimester Proteins [FDR Adjusted *P* Values < 0.05]

UniProtKB ID	14–18 WG vs. 19–20 WG	
	%Δ	*P* FDR
G3XAM2_HUMAN	+173	<0.001
DAG1_HUMAN	+196	0.003
LV106_HUMAN	+249	0.003
PCSK1_HUMAN	+128	0.003
A0A087WZW8_HUMAN	+146	0.003
A0A087WYL9_HUMAN	+81	0.004
A0A087X130_HUMAN	+80	0.008
PTGDS_HUMAN	+435	0.008
ZA2G_HUMAN	+228	0.008
C9JEV0_HUMAN	+223	0.010
A0A087WV47_HUMAN	+147	0.012
APOE_HUMAN	+127	0.012
NRCAM_HUMAN	+142	0.016
FAM3C_HUMAN	+212	0.016
A0A075B6K9_HUMAN	+128	0.019
OSTP_HUMAN	+353	0.019
A0A0A0MS08_HUMAN	+119	0.019
ANT3_HUMAN	+199	0.019
A0A087X1C7_HUMAN	+157	0.028
VTDB_HUMAN	+135	0.028
H0Y7L5_HUMAN	+133	0.030
A0A087X010_HUMAN	+120	0.031
PEDF_HUMAN	+100	0.035
PRS35_HUMAN	+409	0.036
A0A075B6N8_HUMAN	+262	0.044
KV302_HUMAN	+170	0.044
CYTC_HUMAN	+238	0.045
A0A087WXC3_HUMAN	+108	0.045

xylene, and coverslipped using a permanent mounting media. The immunostained slides were examined on a Zeiss Axioskop bright-field microscope (Carl Zeiss, Inc., Thornwood, NY, USA). The images were acquired using a Spot II digital camera (Diagnostics Instruments, Inc., Sterling Heights, MI, USA).

RESULTS

Mass spectrometry identified 1217 proteins (Supplementary Table S1) in at least two independent vitreous samples when all subjects (from 14 WG to 28 years of age) were considered. After quantile normalization and variance filtering, 206 proteins remained.

Human Fetal Vitreous Compared to Young Adult

Samples were divided into dichotomous age groups, embryonic (14–20 WG) and young adult (12, 14, 15, and 28 years old), and the proteomes were compared. Forty-seven proteins (23%) were differentially expressed between the embryonic and young adult vitreous. All of these identified proteins had peptide count values that were significantly lower in the embryonic vitreous, with the fold change ranging from 1.5 to 11 times lower in the embryonic vitreous; the average fold change was 3 times lower (Table 1).

Fetal Vitreous Changes From 14 to 20 WG

Early (14–18 WG) and late (19–20 WG) second-trimester age groups were also compared using a general linear model of the

manufacturer's recommendation using an antibody diluent with background reducer (Dako) and incubated on the sections for 1 hour. Horseradish peroxidase-conjugated goat anti-rabbit secondary antibody (Dako) was applied to the sections and allowed to incubate for one-half hour. The brown-colored enzyme product was developed using a 3,3′-diaminobenzidine (DAB) chromogen (Dako) for 5 minutes. The sections were counterstained using Mayer's hematoxylin (Dako) for 30 seconds, washed in distilled water, then dehydrated in ascending graded ethanol baths, cleared in

TABLE 3. Vitreous Proteins That Decreased When Comparing Early (14–18 WG) Versus Late (19–20 WG) Second-Trimester Proteins [FDR Adjusted P Values < 0.05]

	14–18 WG vs. 19–20 WG	
UniProtKB ID	**%Δ**	**P FDR**
HNRPD_HUMAN	−52	0.008
PRDX5_HUMAN	−69	0.010
COF1_HUMAN	−59	0.011
A8MX94_HUMAN	−54	0.018
TAGL2_HUMAN	−59	0.019
CAPZB_HUMAN	−52	0.026
ROA2_HUMAN	−70	0.031
ENOA_HUMAN	−73	0.044
CAZA1_HUMAN	−56	0.045

log values from the normalized data; 37/206 (18.0%) proteins were statistically different between early versus late age groups using a BH-corrected P value ($P < 0.05$) and had a fold change that ranged from 0.27 to 5.35. Table 2 lists those proteins that increased and Table 3 lists those that decreased when comparing early (14-18 WG) to late (19-20 WG) second trimester.

Spearman's rank correlation of the total peptide counts (all proteins) showed that there was no statistically significant ($R = 0.37$, $P < 0.15$) increase or decrease in overall proteins from 14 to 20 WG. Analysis of changes in individual proteins showed that there was a significant increase or decrease in quantile-normalized peptide spectral counts from 14 to 20 WG (BH FDR $P < 0.05$) in 30.1% (62/206) of proteins (Table 4). Of note, each protein found to decrease from 14 to 20 WG by Spearman's rank correlation analysis was also found to be

TABLE 4. Spearman's Correlation of Vitreous Protein Counts With Embryonic Ages (14-20 WG, $n = 17$)

| Positive Correlations, Increased Expression			Negative Correlations, Decreased Expression		
UniProtKB ID	**ρ**	**P FDR**	**UniProtKB ID**	**ρ**	**P FDR**
PTGDS_HUMAN	0.873	0.001	PRDX5_HUMAN	−0.799	0.005
PRS35_HUMAN	0.815	0.005	6PGD_HUMAN	−0.731	0.009
LUM_HUMAN	0.807	0.005	A8MX94_HUMAN	−0.729	0.009
OSTP_HUMAN	0.806	0.005	ROA2_HUMAN	−0.704	0.012
B4GA1_HUMAN	0.796	0.005	TAGL2_HUMAN	−0.689	0.013
DKK3_HUMAN	0.785	0.006	ENOA_HUMAN	−0.688	0.013
FHR1_HUMAN	0.780	0.006	LDHB_HUMAN	−0.679	0.014
A1AG2_HUMAN	0.777	0.006	1433E_HUMAN	−0.669	0.016
A0A0B4J1Z6_HUMAN	0.770	0.006	ACTG_HUMAN	−0.666	0.017
RARR2_HUMAN	0.766	0.006	HNRPD_HUMAN	−0.666	0.017
A0A075B6K9_HUMAN	0.760	0.006	COF1_HUMAN	−0.638	0.026
KV302_HUMAN	0.755	0.006	CAPZB_HUMAN	−0.625	0.030
A0A087WYL9_HUMAN	0.753	0.006	ALDR_HUMAN	−0.614	0.034
DAG1_HUMAN	0.753	0.006	H0YJG0_HUMAN	−0.613	0.034
LV106_HUMAN	0.753	0.006	1433T_HUMAN	−0.603	0.039
CADH2_HUMAN	0.745	0.007	CAZA1_HUMAN	−0.596	0.041
A0A075B6N8_HUMAN	0.739	0.008	IF4A2_HUMAN	−0.579	0.049
B2MG_HUMAN	0.728	0.009			
A0A087X130_HUMAN	0.725	0.009			
PCSK1_HUMAN	0.724	0.009			
NRCAM_HUMAN	0.722	0.009			
KV102_HUMAN	0.713	0.011			
G3XAM2_HUMAN	0.706	0.012			
ZA2G_HUMAN	0.704	0.012			
A0A087WXC3_HUMAN	0.701	0.012			
FAM3C_HUMAN	0.699	0.012			
SCG1_HUMAN	0.694	0.013			
A1AG1_HUMAN	0.693	0.013			
C9JEV0_HUMAN	0.692	0.013			
KV104_HUMAN	0.691	0.013			
A0A087WZW8_HUMAN	0.686	0.013			
CYTC_HUMAN	0.683	0.014			
PEDF_HUMAN	0.677	0.015			
A0A087X1C7_HUMAN	0.672	0.016			
A0A0A0MS08_HUMAN	0.661	0.018			
A0A087WV47_HUMAN	0.657	0.019			
C9JC84_HUMAN	0.635	0.027			
K1C14_HUMAN	0.629	0.029			
F8VZY9_HUMAN	0.622	0.031			
IGHG2_HUMAN	0.617	0.033			
A0A087X010_HUMAN	0.611	0.034			
VTDB_HUMAN	0.599	0.040			
PGBM_HUMAN	0.594	0.042			
ANT3_HUMAN	0.582	0.049			
CO4A_HUMAN	0.581	0.049			
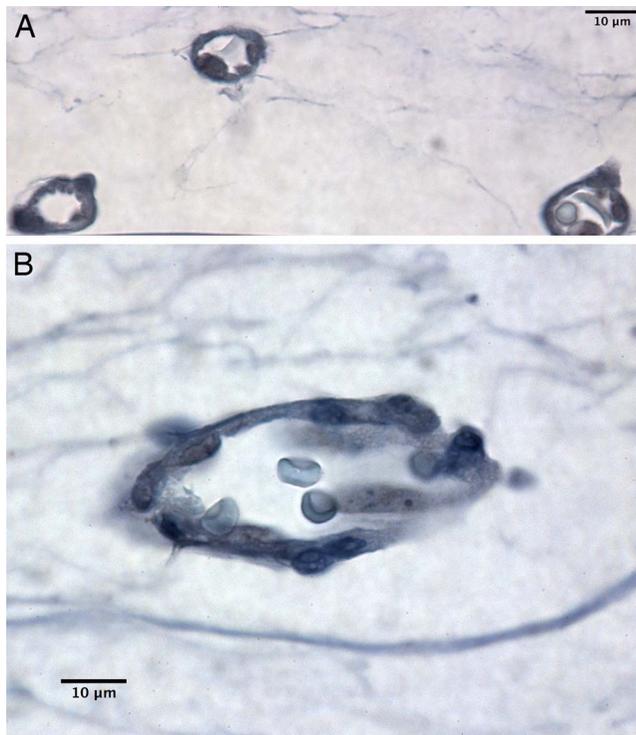
FIGURE 1. Immunohistochemistry in a 14 WG human vitreous demonstrates that clusterin was not detected in the hyaloid vessels (**A**) and cadherin was not detected in the endothelial cells of the hyaloid vessels (**B**). *Scale bar*: 10 µm.

FIGURE 2. Immunohistochemistry in an 18 WG human vitreous demonstrates that positive staining for clusterin in the hyaloid vessels (**A**) and cadherin was detected in the endothelial cells of the hyaloid artery (**B**). This immunostaining pattern confirmed the results of proteomics analysis, which showed that clusterin and cadherin increased from 14 to 20 WG. *Scale bar*: 10 µm.

decreased by the grouped (14–18 vs. 19–20 WG) analysis described above. The same was true for each protein that increased during 14 to 20 WG, confirming these results.

Of these 62, 45 (72.6%) proteins had increased expression during this period of gestation ($R > 0.58$, BH FDR $P < 0.05$). Notable in this group is cadherin (cadh2) ($R = 0.745$, $P \leq 0.008$), which is important for cell adhesion.[34] Pigment epithelium-derived factor (PEDF), which has been shown to be important in antiangiogenesis,[14,35-38] was also found to increase significantly with fetal age from 14 to 20 WG ($R = 0.677$, $P < 0.015$). Cytochrome C (cytc), a known mediator of developmental apoptosis,[39] had increased expression ($R = 0.683$, $P < 0.014$), as did dystroglycan (dag1), the laminin binding component of the dystrophin-glycoprotein complex[40] ($R = 0.753$, $P < 0.007$).

Of the 62 proteins with levels that changed significantly from 14 to 20 WG, 17 (27.4%) had decreased expression ($R < -0.580$, BH FDR $P < 0.05$). Notable proteins that decreased were cofilin-1 (cof1; $R = -0.638$, BH FDR $P < 0.026$), which has been shown to promote/mediate angiogenesis,[41] peroxiredoxin (prdx5; $R = -0.799$, $P < 0.005$), which may play an antioxidant protective role,[42] and glycolytic enzyme enolase[43] (enoa; $R = -0.688$, $P < 0.013$).

Immunohistochemistry

Immunohistochemistry studies confirmed the presence of dystroglycan, clusterin, and cadherin, all shown to have a significant difference in expression in human embryonic vitreous. Positive staining was localized in hyalocytes and hyaloid vessels. Clusterin and cadherin were not detected in 14 WG vitreous cells or structures (Figs. 1A, 2A) but did appear in the hyaloid vasculature by 18 WG (Figs. 1B, 2B). This is consistent with the increase in protein concentrations
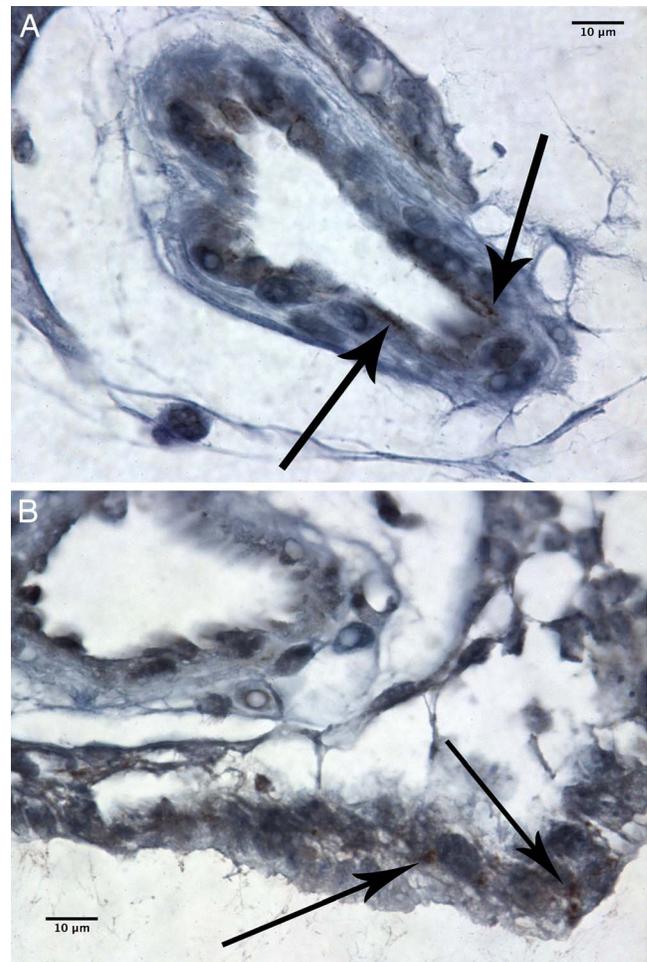
detected in the proteomic analyses (see above). Dystroglycan was detected in the hyaloid vessels of all five embryonic eyes (10, 14, 18 WG; Fig. 3). Immunohistochemical detection of these proteins in hyalocytes and in hyaloid vessels of human embryos suggests that at least these particular proteins that were detected by proteomics originated from vitreous or structures within the vitreous body. This same approach of confirming proteomics with IHC has been previously been employed by others to study hyaloid vessel regression in the mouse.[8]

DISCUSSION

Proteomic investigation of vitreous composition in 14 to 20 WG human embryos and young adult human eyes revealed a complex tissue with 1217 detectable proteins, of which 206 were quantile normalized and variance filtered. While many of these are likely native to vitreous, especially in the embryo, many may also arise from adjacent tissues such as the vascular and neuronal elements of the retina and ciliary body. A review of previously reported human vitreous proteins identified 545 nonredundant proteins.[25] A recent high-resolution Fourier transform study of the normal human vitreous proteome
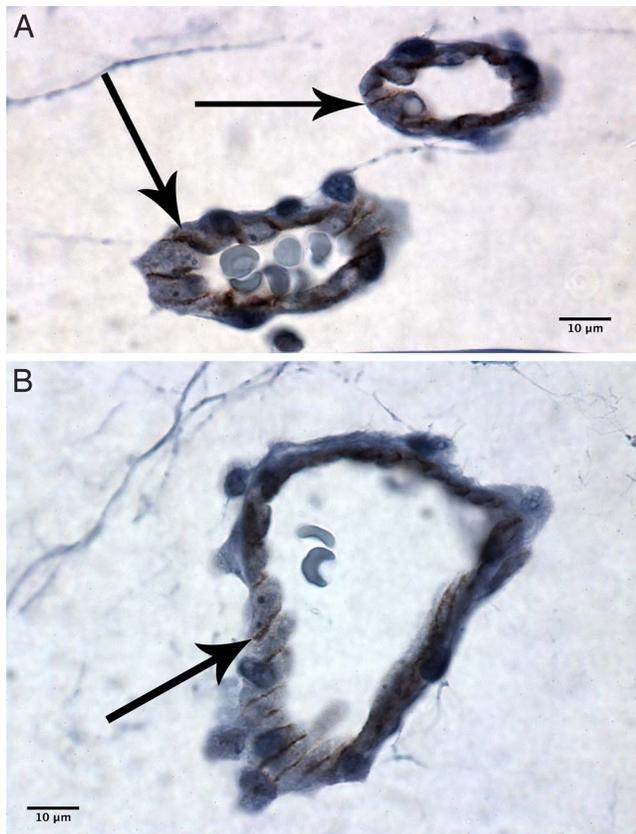
FIGURE 3. Immunohistochemistry for dystroglycan demonstrates positive staining localized to the cell junctions of the hyaloid vascular endothelium in a 14 WG (**A**) and an 18 WG (**B**) human embryo. *Scale bar*: 10 μm.

FIGURE 4. Venn diagram comparing the proteomes of three human vitreous studies (present study versus Murthy et al.[26] versus Semba et al.[25]).

identified 1205 proteins, 682 (57%) of which had not been previously described in vitreous.[26] The study reported herein identified 1217 vitreous proteins, 744 (61%) of which had not been previously reported in either of the aforementioned studies (Fig. 4).

The protein composition of human embryonic vitreous differs from young adult vitreous and changes significantly from 14 to 20 WG, during the second trimester of gestation. This occurs concurrently with regression of embryonic vitreous vessels as well as other developmental changes in the eye. Of the 206 quantile-normalized/variance-filtered proteins identified in human fetal vitreous, 37 (18%) showed a significant change in expression from 14 to 20 WG (early to late second trimester). Some of these, such as PEDF and cofilin-1, are known to be important in angiogenesis and may be critically involved in this and one or more other processes of vitreous or ocular embryogenesis. Thus, it is intriguing to postulate that some of the changes detected in the proteomic profile of human fetal vitreous during the second trimester are related to the regression of the embryonic vitreous vasculature, although other developmental events are also occurring during this period. In this context, a better understanding of hyaloid vasculature regression may prove useful in developing new therapies for vasoproliferative eye diseases, metastatic carcinomas, and others. To this end, the proteins identified in this study, especially those shown to change in concentration and those corroborated in previous studies, may be worth exploring as potential avenues for new therapeutic approaches to both stimulate endogenous inhibitory pathways and
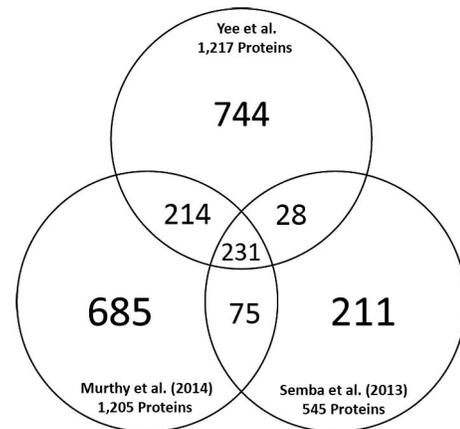
suppress stimulatory pathways in the management of neovascular pathologies.

A similar proteomic study was undertaken in the developing mouse vitreous using two-dimensional gel electrophoresis (2DE), a distinctly different methodology than that employed in the present study.[8] Furthermore, the mouse specimens consisted of lens with pupillary membrane, tunica vasculosa lentis, and vasa hyaloidea propria, while the specimens in the present study were purely vitreous. This may explain why only a small number of proteins were found in both mouse and human proteomes. This and contradictory findings regarding changes from early to late fetal stages are possibly due to different methodologies as well as species differences.

Future studies should explore the fetal human proteome in search of "missing proteins"[44] with the findings validated by multiple reaction monitoring (MRM) methodologies, as has been previously described.[45]

References

1. Sebag J. Embryology of the vitreous. In: Sebag J. *The Vitreous: Structure, Function, and Pathobiology*. New York: Springer-Verlag; 1989:7–14.

2. Kingston ZS, Provis JM, Madigan MC. Development and developmental disorders of vitreous. In: Sebag J, ed. *Vitreous: In Health and Disease*. New York: Springer; 2014; 2014:95–111.

3. Saint-Geniez M, D'Amore PA. Development and pathology of the hyaloid, choroidal and retinal vasculature. *Int J Dev Biol*. 2004;48:1045–1058.

4. Bremer FM, Rasquin F. Histochemical localization of hyaluronic acid in vitreous during embryonic development. *Invest Ophthalmol Vis Sci*. 1998;39:2466–2469.

5. Bishop PN. Structural macromolecules and supramolecular organisation of the vitreous gel. *Prog Retin Eye Res*. 2000;19:323–344.

6. Sebag J. Molecular biology of pharmacologic vitreolysis. *Trans Am Ophthalmol Soc*. 2005;103:473–494.

7. Sebag J, Yee KMP. Vitreous: from biochemistry to clinical relevance. In: Tasman W, Jaeger EA, eds. *Duane's Foundations of Clinical Ophthalmology*. Philadelphia: Lippincott Williams & Wilkins; 2007:1–67.

8. Albè E, Chang JH, Azar NF, Ivanov AR, Azar DT. Proteomic analysis of the hyaloid vascular system regression during ocular development. *J Proteome Res*. 2008;7:4904–4913.

9. Albè E, Escalona E, Rajagopal R, Javier JA, Chang JH, Azar DT. Proteomic identification of activin receptor-like kinase-1 as a differentially expressed protein during hyaloid vascular system regression. *FEBS Lett*. 2005;579:5481–5486.

10. Cryan LM, O'Brien C. Proteomics as a research tool in clinical and experimental ophthalmology. *Proteomics Clin Appl*. 2008;2:762–775.

11. Shimizu A, Nakanishi T, Koyama R, Ikeda T. Proteomics in clinical research: new approach of mass spectrometry. *Rinsho Byori*. 2002;50:169–172.

12. Kim T, Kim SJ, Kim K, et al. Profiling of vitreous proteomes from proliferative diabetic retinopathy and nondiabetic patients. *Proteomics*. 2007;7:4203–4215.

13. Shitama T, Hayashi H, Noge S, et al. Proteome profiling of vitreoretinal diseases by cluster analysis. *Proteomics Clin Appl*. 2008;2:1265–1280.

14. Ouchi M, West K, Crabb JW, Kinoshita S, Kamei M. Proteomic analysis of vitreous from diabetic macular edema. *Exp Eye Res*. 2005;81:176–182.

15. Patz A, Brem S, Finkelstein D, et al. A new approach to the problem of retinal neovascularization. *Ophthalmology*. 1978;85:626–637.

16. Gao BB, Chen X, Timothy N, Aiello LP, Feener EP. Characterization of the vitreous proteome in diabetes without diabetic retinopathy and diabetes with proliferative diabetic retinopathy. *J Proteome Res*. 2008;7:2516–2525.

17. Yamane K, Minamoto A, Yamashita H, et al. Proteome analysis of human vitreous proteins. *Mol Cell Proteomics*. 2003;2:1177–1187.

18. Kim SJ, Jin J, Kim YJ, Kim Y, Yu HG. Retinal proteome analysis in a mouse model of oxygen-induced retinopathy. *J Proteome Res*. 2012;11:5186–5203.

19. Yoshimura T, Sonoda KH, Sugahara M, et al. Comprehensive analysis of inflammatory immune mediators in vitreo-retinal diseases. *PLoS One*. 2009;4:e8158.

20. Nakanishi T, Koyama R, Ikeda T, Shimizu A. Catalogue of soluble proteins in the human vitreous humor: comparison between diabetic retinopathy and macular hole. *J Chromatog B*. 2002;776:89–100.

21. Koyama R, Nakanishi T, Ikeda T, Shimizu A. Catalogue of soluble proteins in human vitreous humor by one-dimensional sodium dodecyl sulfate-polyacrylamide gel electrophoresis and electrospray ionization mass spectrometry including seven angiogenesis-regulating factors. *J Chromatog B*. 2003;792:5–21.

22. Kim SJ, Kim S, Park J, et al. Differential expression of vitreous proteins in proliferative diabetic retinopathy. *Curr Eye Res*. 2006;31:231–240.

23. García-Ramírez M, Canals F, Hernández C, et al. Proteomic analysis of human vitreous fluid by fluorescence-based difference gel electrophoresis (DIGE): a new strategy for identifying potential candidates in the pathogenesis of proliferative diabetic retinopathy. *Diabetologia*. 2007;50:1294–1303.

24. Wang H, Feng L, Hu JW, Xie CL, Wang F. Characterisation of the vitreous proteome in proliferative diabetic retinopathy. *Proteome Sci*. 2012;10:15.

25. Semba RD, Enghild JJ, Venkatraman V, Dyrlund TF, Van Eyk JE. The Human Eye Proteome Project: perspectives on an emerging proteome. *Proteomics*. 2013;13:2500–2511.

26. Murthy KR, Goel R, Subbannayya Y, et al. Proteomic analysis of human vitreous humor. *Clin Proteomics*. 2014;11:29.

27. Gao BB, Phipps JA, Bursell D, Clermont AC, Feener EP. Angiotensin AT1 receptor antagonism ameliorates murine retinal proteome changes induced by diabetes. *J Proteome Res*. 2009;8:5541–5549.

28. Nesvizhskii AI, Keller A, Kolker E, Aebersold R. A statistical model for identifying proteins by tandem mass spectrometry. *Anal Chem*. 2003;75:4646–4658.

29. Ashburner M, Ball CA, Blake JA, et al. Gene ontology: tool for the unification of biology. The Gene Ontology Consortium. *Nat Genet*. 2000;25:25–29.

30. Benjamini Y, Hochberg Y. Controlling the false discovery rate: a practical and powerful approach to multiple testing. *J R Statist Soc B*. 1995;57:289–300.

31. Pan BX, Yee KM, Ross-Cisneros FN, Sadun AA, Sebag J. Inner retinal optic neuropathy: vitreomacular surgery-associated disruption of the inner retina. *Invest Ophthalmol Vis Sci*. 2014;55:6756–6764.

32. Ross-Cisneros FN, Pan BX, Silva RA, et al. Optic nerve histopathology in a case of Wolfram Syndrome: a mitochondrial pattern of axonal loss. *Mitochondrion*. 2013;13:841–845.

33. La Morgia C, Ross-Cisneros FN, Sadun AA, et al. Melanopsin retinal ganglion cells are resistant to neurodegeneration in mitochondrial optic neuropathies. *Brain*. 2010;133(pt 8):2426–2438.

34. Lambeng N, Wallez Y, Rampon C, et al. Vascular endothelial-cadherin tyrosine phophorylation in angiogenic and quiescent adult tissues. *Circ Res*. 2005;96:384–391.

35. Ohno-Matsui K. Molecular mechanism for choroidal neovascularization in age-related macular degeneration. *Nihon Ganka Gakkai Zasshi*. 2003;107:657–673.

36. Haurigot V, Villacampa P, Ribera A, et al. Long-term retinal PEDF overexpression prevents neovascularization in a murine adult model of retinopathy. *PLoS One*. 2012;7:e41511.

37. Bhutto IA, McLeod DS, Hasegawa T, et al. Pigment epithelium-derived factor (PEDF) and vascular endothelial growth factor (VEGF) in aged human choroid and eyes with age-related macular degeneration. *Exp Eye Res*. 2006;82:99–110.

38. Huber M, Wachtlin J. Vitreous levels of proteins implicated in angiogenesis are modulated in patients with retinal or choroidal neovascularization. *Ophthalmologica*. 2012;228:188–193.

39. Liu X, Kim CN, Yang J, Jemmerson R, Wang X. Induction of apoptotic program in cell-free extracts: requirement for dATP and cytochrome c. *Cell*. 1996;86:147–157.

40. Ibraghimov-Beskrovnaya O, Ervasti JM, Leveille CJ, Slaughter CA, Sernett SW, Campbell KP. Primary structure of dystrophin-associated glycoproteins linking dystrophin to the extracellular matrix. *Nature*. 1992;355:696–702.

41. Keezer SM, Ivie SE, Krutzsch HC, Tandle A, Libutti SK, Roberts DD. Angiogenesis inhibitors target the endothelial cell cytoskeleton through altered regulation of heat shock protein 27 and cofilin. *Cancer Res*. 2003;63:6405–6412.

42. Rhee S, Chae H, Kim K. Peroxiredoxins: a historical overview and speculative preview of novel mechanisms and emerging concepts in cell signaling. *Free Radic Biol Med*. 2005;38:1543–1552.

43. Pancholi V. Multifunctional alpha-enolase: its role in diseases. *Cell Mol Life Sci*. 2001;58:902–920.

44. Lane L, Bairoch A, Beavis RC, et al. Metrics for the Human Proteome Project 2013-2014 and strategies for finding missing proteins. *J Proteome Res*. 2014;13:15–20.

45. Kitata RB, Dimayacyac-Esleta BR, Choong WK, et al. Mining missing membrane proteins by high-pH reverse-phase Stage-Tip fractionation and multiple reaction monitoring mass spectrometry. *J Proteome Res*. 2015;14:3658–3669.